Current Biology, Volume *19*

Supplemental Data

Buildup of Choice-Predictive Activity

in Human Motor Cortex

during Perceptual Decision Making

Tobias H. Donner, Markus Siegel, Pascal Fries, and Andreas K. Engel

Supplemental Experimental Procedures

Stimuli

The dynamic random dot patterns were constructed offline in MATLAB (MathWorks Inc., Massachusetts, USA) and presented using the Presentation Software (NeuroBehavioral Systems, Albany, CA, USA). Stimuli were projected from a calibrated LCD projector outside of the magnetically shielded room onto a back projection screen in front of the subject's head. The refresh rate of the projector was 60 Hz. Each frame of the animation consisted of an array of white dots randomly positioned on a black background. Each dot was displaced from frame to frame. *Noise* patterns ("target absent") consisted only of dots that were randomly displaced from frame to frame. *Signal + noise* patterns ("target present") contained a small fraction of dots that were coherently displaced in a common direction, with fixed spatial offset. All other dots were displaced randomly. The coherently moving dots were randomly selected afresh on each new frame (limited "life-time"). The motion coherence (i.e., the fraction of coherently moving dots) was chosen individually for each subject to correspond to the 71% correct detection threshold, as determined by the method of constant stimuli. The patterns were confined to a circular aperture and centered on a red fixation cross in the center of the screen. The diameter of each of the dots on the projection screen was ~0.2 deg. Their density and speed were ~1.7 deg^{-2} and ~11.5 deg per s, respectively. The aperture diameter was ~43 deg.

Task and Procedure

Subjects performed a "yes/no" motion coherence detection task (Figure 1). The target signal occurred on 50% of the trials. Subjects were instructed to fixate the crosshair throughout the trial, monitor the stimulus pattern, form a decision about the target presence, and report this decision by pressing one of two response buttons ("yes/no") with their left or right index finger after the delay, prompted by the fixation cross offset. Auditory feedback (a beep) was provided after each incorrect response. The subsequent inter-trial-interval (not shown in Figure 1A) spanned 900 ms. Subjects were allowed to make eye movements or blinks during the inter-trial-interval. Target absence/presence was randomly selected on each trial, under the constraint that each would occur equally often within a run. If present, the target signal moved either upward or downward, under the constraint that both directions would occur equally often within a run. Apart from these variations, all stimulus patterns were exact repeats. After blocks of 50 trials,

subjects were allowed to pause, without moving their heads. They initiated the start of each new trial block by a button press. Each run consisted of 400 trials and lasted about 50 min.

Data Analysis

Trials containing eye blinks, saccades, muscle artifacts and signal jumps were rejected from further analysis. Line-noise was removed by subtracting the 50, 100, 150 and 200 Hz Fourier components of the individual epochs. Data were then re-sampled at 600 Hz and submitted to spectral analysis, using the "multi-taper" technique [1].

To isolate effector-selective MEG-activity, we calculated time-frequency representations of the MEG power (spectrograms) of each sensor and trial, using a sliding window Fourier transform (250 ms window, 25 ms window step-size, 16 Hz spectral smoothing, 2 Hz frequency bins). We calculated separate spectrograms aligned to stimulus onset and to button press. The spectrograms were converted into percent power change relative to the average pre-stimulus baseline (0.5 s before stimulus onset). These normalized spectrograms were averaged across trials, separately for right- and left-hand button presses, across two groups of twelve sensors overlying the left and right motor cortices, and across subjects (Figure 2A). Analogous to the calculation of the lateralized readiness potential [2], frequency-specific activity ipsilateral to the button press was subtracted from the activity contralateral to the button press. The differential activity was collapsed across left- and right-hand button presses and across subjects, providing a simple measure of effector-selective activity (Figure 2B).

We used an adaptive spatial filtering technique called "linear beamforming" [3, 4] to reconstruct effector-selective 12-36 Hz and 64-100 Hz activities in cortical source space. This technique estimates the frequency- and location-specific power in source space by applying linear filters $\mathbf{A}(\mathbf{r},f)$ to the sensor-level MEG data, separately for each location of interest $\mathbf{r}$ and frequency range of interest f:

$$\mathbf{A}(\mathbf{r},f) = (\mathbf{L}^T(\mathbf{r})\mathbf{C}\,(f)^{-1}\mathbf{L}(\mathbf{r}))^{-1}\mathbf{L}^T(\mathbf{r})\mathbf{C}(f)^{-1}, \quad (1)$$

where the columns of $\mathbf{L}(\mathbf{r})$ contain the lead fields (i.e., the mapping from source space to sensor space) for two orthogonal tangential dipoles at location $\mathbf{r}$, and $\mathbf{C}$ denotes the cross-spectral-density matrix of the sensor-level MEG data in the frequency range of interest. This filter passes band-limited activity from $\mathbf{r}$ with unit gain, while maximally suppressing the activity from all other sources [3, 4]. The estimates of spectral power were computed according to:

$$P(\mathbf{r},f) = \lambda_1(\mathbf{A}(\mathbf{r},f)\mathbf{C}(f)\mathbf{A}^{*T}(\mathbf{r},f)), \quad (2)$$

where λ_1 denotes the largest singular value of the cross-spectrum estimates of two orthogonal tangential dipoles at location $\mathbf{r}$. Thus, λ_1 is the power of a dipole pointing into the dominant direction at $\mathbf{r}$ [4].

We used this spatial filtering technique to reconstruct the cortical distribution of effector-selective activity before movement execution, by contrasting activity in the 12-36 Hz and 64-100 Hz bands between left and right hand button presses. Activity was expressed as the band-limited power during the 0.5 s before button press, normalized by the band-limited power during baseline (0.5 s before stimulus onset). The source space was divided into a regular grid of 7.5 x 7.5 x 7.5 mm resolution covering the cerebral cortex. Within each run, ensembles of activity maps were computed for each behavioral response (left-hand/right-hand), each map leaving out one different trial; maps of the mean activity per grid point, and the standard error of the mean, were then computed by means of a jackknife procedure [5]. These maps were converted into statistical t-maps (left vs. right hand), linearly interpolated to a 1 mm^3 grid, converted into z-maps, and pooled across runs (within subjects) according to:

$$\bar{Z} = \frac{1}{\sqrt{N}} \sum_{i=1}^{i=N} Z_i, \quad (3)$$

where *i* denotes trial and *N* is the total number of trials. The resulting z-maps were morphed onto the MNI template brain based on the individual structural MRIs using the SPM2 (http://www.fil.ion.ucl.ac.uk/ spm/software/spm2/) non-linear warping algorithm, and then pooled across subjects, again using eq. (3).

To reconstruct the time courses of effector-selective band-limited activity aligned to stimulus onset (Figure 3), we again used the spatial filtering technique described above (eq. (1) and (2)). Now, we focused on four cortical regions of interest, which were defined on the individual MRIs: The anterior portion of PMd, the hand area within M1, visual cortical area MT, and a region in dorsolateral prefrontal cortex. We defined the M1 hand area based on an established anatomical landmark, an omega-shaped formation of the dorsal part of the central sulcus [6]. The PMd region of interest was positioned in the anterior portion of premotor cortex [7], located in the junction of the precentral and the superior frontal sulcus, about 1.5 cm anterior to the M1 region. The MT region of interest was defined based on a combination of anatomical landmarks and fMRI responses in standard MT-localizer scans, which were performed in three of the four subjects: The human MT+ complex is located in the junction of the ascending limb of the inferior temporal sulcus with its posterior continuation [8]; these anatomical criteria were in close correspondence with the maps of fMRI responses. The prefrontal cortex region of interest was placed at the anterior end of the posterior third of the medial frontal gyrus.

We reconstructed the time courses of band-limited activity in each of these regions by calculating separate filters for the 12-36 Hz and 64-100 Hz bands and for three trial intervals: baseline (-0.5-0 s relative to stimulus onset), stimulus viewing (0-2 s relative to stimulus onset), and delay (2-2.5 s relative to stimulus onset). These filters were applied to the time- and frequency-specific cross-spectral density matrices of the sensor-level MEG data (see eq. (2)), estimated by means of multi-taper Fourier transform. Specifically, for both frequency bands, cross-spectral density matrices were calculated for 500 ms time windows aligned to stimulus onset and sliding across the trial in steps of 125 ms. We calculated the lateralization of MEG-activity as the difference between log-transformed power contralateral vs. ipsilateral to the hand indicating "yes". For each of the four trial categories, we subtracted the mean baseline lateralization (most likely reflecting confounding factors and not the decision process) from the corresponding single-trial time courses.

Choice-predictive MEG-activity in both areas and frequency bands was analyzed according to two schemes. In a first scheme (Figure 3A), we used ROC-analysis [9, 10] to quantify the reliability of choice-predictive lateralization of activity. The analysis measured the overlap of the single-trial distributions of lateralization (contralateral - ipsilateral to "yes-button") before "yes" and "no" choices ("choice probability"), separately for correct and incorrect choices, combining all trials across subjects. We used a two-tailed permutation test [5] with 10^3 permutations to test the choice probability for significant deviation from 0.5 chance level. In a second scheme (Figure 3B), we analyzed the lateralization separately for the four trial categories. For each category, we tested the deviation from zero baseline lateralization by means of a t-test, again combining trials across subjects, and converted the resulting t-scores into z-scores.

We used the following procedure to analyze the correlation between the temporal integral of gamma-band activity in MT and the choice-predictive lateralization in M1 (Figure 4). For each time point *t* (ranging from -0.25 to 2.25 s relative to stimulus onset in steps of 125 ms), we averaged the single-trial estimates of MT activity in the 64-100 Hz range across both

hemispheres, and summed this across the stimulus interval, up to *t*. Spontaneous fluctuations of neural population activity contain spatially widespread components, which are unrelated to local neuronal representations [11-13]. Such "global" activity components were removed from the effector-selective M1 activity by taking the difference between hemispheres (see above). We used orthogonal projection to remove the global activity components from the single-trial estimates of MT activity, by subtracting exactly the component that these estimates shared with the single-trial estimates for a distant "reference" region [11, 12]. The dorsolateral prefrontal cortex region served as a reference for the results described in the paper. Qualitatively identical results were obtained from using different reference regions (e.g. in parietal cortex). The integrated single-trial MT activity up to *t* and the single-trial M1 lateralization (contralateral - ipsilateral to "yes-button") at *t* were z-transformed within the four stimulus-report conditions, combined across conditions and subjects, binned by the MT integral, and correlated. Figure 4A shows this analysis for $t = 2$ s, that is, the last time point of the stimulus interval. Figure 4B shows the correlation as a function of *t*. To verify that the statistical significance of the correlation did not depend on the binning of trials by MT activity we repeated the analysis without binning and for several bin sizes from 50 to 500 (in steps of 50). As expected, the correlation coefficients decreased with bin size, but they were highly significant ($p < 0.01$) without binning and across bin sizes.

Spectral Signature of Effector-Selective Activity before Button Press

To characterize the spectral signature of the effector-selective activity before movement execution in more detail, we calculated spectra of the MEG activity in the 0.5 s before button press, analogous to the time-frequency representations in Figure 2, but with finer spectral resolution (multi-taper Fourier transform, 6 Hz spectral smoothing). These spectra exhibited two distinct peaks of effector-selective activity in the range below 40 Hz: One in the alpha-band (8-12 Hz) and another in the beta-band (12-36 Hz) (Figure S1). Both components were bilaterally suppressed before left and right hand movements (Figure S1A), but more strongly before contralateral than before ipsilateral movements (Figure S1B). This effector-selective lateralization was stronger in the beta-band (Figure S1B). Similar patterns of alpha- and beta-band suppression have consistently been observed in previous electrophysiological studies of motor preparation in humans [14-20].

Effector-selective (contralateral > ipsilateral) activity prior to movement execution was also expressed in the gamma-band, ranging from about 50-100 Hz (Figure S1B). The 64-100 Hz gamma-band used in the source reconstructions of the present study was chosen to exclude a contribution of the widespread stimulus-locked entrainment of MEG activity at 60 Hz driven by the flickering "noise" fraction of the random dot patterns [24].

Movement-related modulations in the gamma-band have consistently been observed in electrocorticogram recordings [16, 18, 20, 21], and, more recently, also in extracranial EEG and MEG recordings [15, 22, 23]. Results from one MEG study suggest that the contralateral gamma-band enhancement begins after movement onset, and may therefore partly reflect afferent somatosensory activity [15]. Our data are consistent with this study in that the strongest transient gamma-band modulation occurred around and after button press (Figure 2). However, in accord with a previous MEG-study of motor preparation [23], we also observed effector-selective gamma-band modulations long before movement execution (Figures 2 and 3).

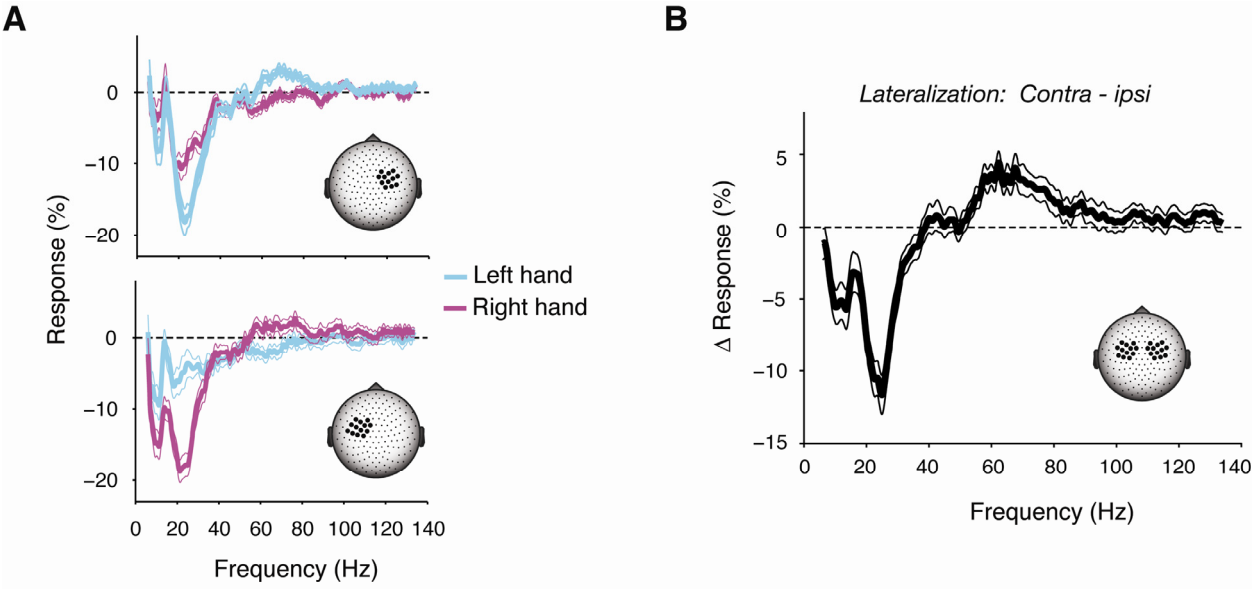

Figure S1.

Figure S1. Spectral Signature of Effector-Selective MEG Activity before Button Press (-0.5 to 0 s)

MEG activity is expressed as percent power change relative to the prestimulus baseline power.

(A) Group average spectra of activity of two symmetric groups of MEG sensors overlying right (upper panel) and left (lower panel) motor cortices, separately for button presses with the left and right hands. Thick lines represent the mean and thin lines the SEM across runs. Sensor groups are marked on schematic scalp projections.

(B) Spectra of the MEG-lateralization, i.e., the difference between the two sensor groups contralateral and ipsilateral to the button press, averaged across both kinds of button presses.

Absence of Choice-Predictive Activity in Control Region

To assess the spatial specificity of the reported choice-predictive activity, we repeated the analysis for a control region in dorsolateral prefrontal cortex located in the medial frontal gyrus (see Supplemental Experimental Procedures: Data Analysis above). The activity of this region showed no hemispheric lateralization before movement execution (Figure 2C). Figure S2 shows the time courses of choice probability for beta- and gamma-band lateralization in this region during stimulus viewing. There was no significant choice-predictive lateralization of activity in prefrontal cortex. As discussed in the main paper, the absence of such activity does not imply that there was no decision-related activity in prefrontal cortex. Rather, it implies that there was no significant *lateralization* of activity reflecting the motor plan to respond with one or the other hand. Thus, just as right before movement execution (Figure 2C), the lateralization during the stimulus interval was specific to regions with a known contralateral motor bias.

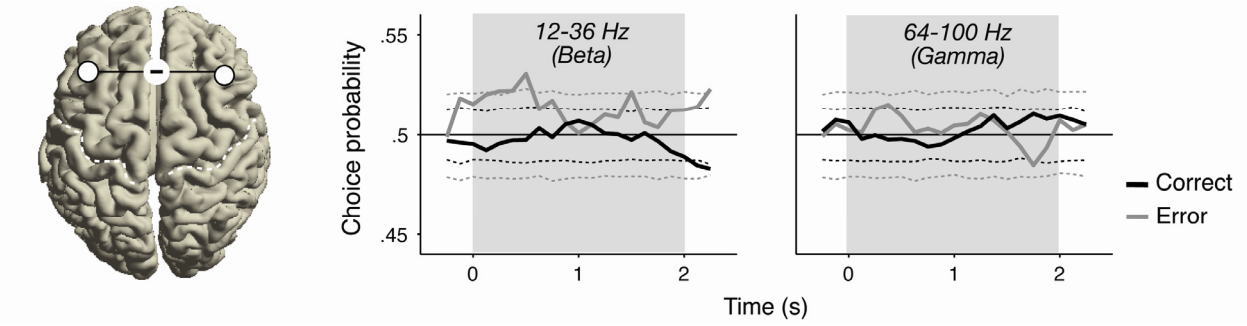

Figure S2. Time Courses of Choice-Predictive Activity in Control Region

Choice probability ("yes" vs. "no") quantifies the predictability of choices from the prefrontal response lateralization (contralateral - ipsilateral to "yes-button"). Time courses are aligned to stimulus onset and shown separately for gamma- and beta-bands, and for correct (black) and incorrect (gray) choices. The solid line at choice probability = 0.5 corresponds to chance level prediction. The dashed black and gray lines indicate significance levels of the corresponding time courses ($p < 0.05$, two-sided permutation test). The light gray shade indicates the stimulus interval. Inset: The regions of interest in the left and right medial frontal gyrus are displayed on a cortical surface reconstruction. The dashed lines indicate the central sulcus.

Supplemental References

1. Mitra, P., and Bokil, H. (2007). Observed Brain Dynamics, (New York: Oxford University Press US).
2. Coles, M.G. (1989). Modern mind-brain reading: psychophysiology, physiology, and cognition. Psychophysiology *26*, 251-269.
3. Gross, J., Kujala, J., Hamalainen, M., Timmermann, L., Schnitzler, A., and Salmelin, R. (2001). Dynamic imaging of coherent sources: Studying neural interactions in the human brain. Proc Natl Acad Sci U S A *98*, 694-699.
4. Van Veen, B.D., van Drongelen, W., Yuchtman, M., and Suzuki, A. (1997). Localization of brain electrical activity via linearly constrained minimum variance spatial filtering. IEEE Trans Biomed Eng *44*, 867-880.
5. Efron, B., and Tibshirani, R. (1998). An introduction to the bootstrap, 1st CRC Press reprint. Edition, (Boca Raton, Fla.: Chapman & Hall/CRC).
6. Yousry, T.A., Schmid, U.D., Alkadhi, H., Schmidt, D., Peraud, A., Buettner, A., and Winkler, P. (1997). Localization of the motor hand area to a knob on the precentral gyrus. A new landmark. Brain *120 Pt 1*, 141-157.
7. Picard, N., and Strick, P.L. (2001). Imaging the premotor areas. Curr Opin Neurobiol *11*, 663-672.
8. Dumoulin, S.O., Bittar, R.G., Kabani, N.J., Baker, C.L., Jr., Le Goualher, G., Bruce Pike, G., and Evans, A.C. (2000). A new anatomical landmark for reliable identification of human area V5/MT: a quantitative analysis of sulcal patterning. Cereb Cortex *10*, 454-463.
9. Green, D.M., and Swets, J.A. (1966). Signal detection theory and psychophysics, (New York: Wiley).
10. Britten, K.H., Newsome, W.T., Shadlen, M.N., Celebrini, S., and Movshon, J.A. (1996). A relationship between behavioral choice and the visual responses of neurons in macaque MT. Vis Neurosci *13*, 87-100.
11. Fox, M.D., Snyder, A.Z., Zacks, J.M., and Raichle, M.E. (2006). Coherent spontaneous activity accounts for trial-to-trial variability in human evoked brain responses. Nat Neurosci *9*, 23-25.
12. Leopold, D.A., Murayama, Y., and Logothetis, N.K. (2003). Very slow activity fluctuations in monkey visual cortex: implications for functional brain imaging. Cereb Cortex *13*, 422-433.
13. Donner, T.H., Sagi, D., Bonneh, Y.S., and Heeger, D.J. (2008). Opposite neural signatures of motion-induced blindness in human dorsal and ventral visual cortex. J Neurosci *28*, 10298-10310.
14. Morash, V., Bai, O., Furlani, S., Lin, P., and Hallett, M. (2008). Classifying EEG signals preceding right hand, left hand, tongue, and right foot movements and motor imageries. Clin Neurophysiol *119*, 2570-2578.
15. Cheyne, D., Bells, S., Ferrari, P., Gaetz, W., and Bostan, A.C. (2008). Self-paced movements induce high-frequency gamma oscillations in primary motor cortex. Neuroimage *42*, 332-342.
16. Pfurtscheller, G., Graimann, B., Huggins, J.E., Levine, S.P., and Schuh, L.A. (2003). Spatiotemporal patterns of beta desynchronization and gamma synchronization in corticographic data during self-paced movement. Clin Neurophysiol *114*, 1226-1236.
17. Crone, N.E., Miglioretti, D.L., Gordon, B., Sieracki, J.M., Wilson, M.T., Uematsu, S., and Lesser, R.P. (1998). Functional mapping of human sensorimotor cortex with electrocorticographic spectral analysis. I. Alpha and beta event-related desynchronization. Brain *121 (Pt 12)*, 2271-2299.
18. Miller, K.J., Leuthardt, E.C., Schalk, G., Rao, R.P., Anderson, N.R., Moran, D.W., Miller, J.W., and Ojemann, J.G. (2007). Spectral changes in cortical surface potentials during motor movement. J Neurosci *27*, 2424-2432.
19. Pfurtscheller, G., and Aranibar, A. (1979). Evaluation of event-related desynchronization (ERD) preceding and following voluntary self-paced movement. Electroencephalogr Clin Neurophysiol *46*, 138-146.
20. Pfurtscheller, G., and Lopes da Silva, F.H. (1999). Event-related EEG/MEG synchronization and desynchronization: basic principles. Clin Neurophysiol *110*, 1842-1857.
21. Crone, N.E., Miglioretti, D.L., Gordon, B., and Lesser, R.P. (1998). Functional mapping of human sensorimotor cortex with electrocorticographic spectral analysis. II. Event-related synchronization in the gamma band. Brain *121 (Pt 12)*, 2301-2315.
22. Ball, T., Demandt, E., Mutschler, I., Neitzel, E., Mehring, C., Vogt, K., Aertsen, A., and Schulze-Bonhage, A. (2008). Movement related activity in the high gamma range of the human EEG. Neuroimage *41*, 302-310.
23. Schoffelen, J.M., Oostenveld, R., and Fries, P. (2005). Neuronal coherence as a mechanism of effective corticospinal interaction. Science *308*, 111-113.
24. Donner, T.H., Siegel, M., Oostenveld, R., Fries, P., Bauer, M., and Engel, A.K. (2007). Population activity in the human dorsal pathway predicts the accuracy of visual motion detection. J Neurophysiol *98*, 345-359.